In-Situ Monitoring of Thin-Film Quality Using Evanescent Microwave Local Imaging Probes with Near-Atomic Resolution

Massood Tabib-Azar *^+, R. Wang *, D. Park *, and S. R. LeClair#

* Electrical Engineering and Computer Science Dept., Macromolecular Science Dept. and Physics Dept., Case Western Reserve University, Cleveland, OH 44106

^ Manufacturing Instrumentation Consultants Company, LLC
Suite # 427, 11000 Cedar Road, Cleveland, Ohio 44106

+ On Sabbatical at: EE Dept., Yale University, New Heaven, CT

Air Force Research Laboratory, Materials & Manufacturing Directorate
Wright-Patterson AFB, OH

Contact e-mail: Massood.Tabib-Azar@yale.edu

Abstract: Local probes, such as scanning tunneling (STM), atomic force (AFM), near-field scanning (NSOM), and evanescent microwave (EMM) microscopes are important material characterization tools with very high spatial resolutions capable of operating in many different environments. All these probes are currently laboratory tools with limited real-time manufacturing applications because of their low speed. Of all these probes, EMM has the greatest potential of acquiring higher scanning speed because it does not require an intimate contact with the material surface. Moreover, EMM is capable of characterizing a variety of organic and inorganic materials including metals, semiconductors, and insulators over a wide range of frequencies and length scales. Here we discuss the application of parallel EMMs (PEMM) in monitoring thin-film quality in real-time and in-situ.

Keywords: Intelligent Sensors, Parallel Probes, Hyperspectral Imaging

1. INTRODUCTION

Local probes, such as atomic force microscope (AFM), scanning tunneling microscope (STM), Near-Field Scanning Optical Microscope (NSOM), and Evanescent Microwave Microscope (EMM), are great laboratory tools with atomic spatial resolutions. There are major efforts in the US [1] to construct parallel local probes with fast imaging speed for manufacturing applications with real-time and in-situ capabilities. Although most of these local probes can be used to perform spectroscopy, their main shortcoming is that the structures they detect cannot be identified readily and some prior knowledge of the "thing" they are detecting is needed. Thus, the main trust in this area, in addition to constructing parallel probes, is to enable the local probes to detect and identify the objects at the surface or subsurface of the sample. This capability is of particular importance in material applications.

Owing to its high operation frequency (0.1-100 GHz) the EMM has the potential of attaining much higher speed than its other relatives and it also has the potential of performing simultaneous measurements at different frequencies, so called hyperspectral measurements, to identify the object it is detecting. The hyperspectral capability of the EMM is also of great importance in enabling it to ultimately deal with probe-to-sample distance, or stand-off, variations which can be a major problem in high scanning speed local probes.

Data interpretation and bandwidth requirement in parallel probes are also important factors. Let us assume that only 10 probes, each with 10 μm spatial resolution, operating in parallel are used to monitor defects in a material strip and that that these probes are located 20 μm from each other so that they cover a strip of 200 μm. The area that they map depends on

the speed of their scan which for the purpose of this example will be assumed to be 1 cm/s. Thus, in one second, they probes cover 1 cm X 0.02 cm = 0.02 cm^2 area. The output of the probes should be sampled such that at least every 5 μm, or 0.5 ms (Nyquist criteria) a reading is obtained. For 10 probes, then, the sampling rate is 20,000 samples/s. Even at 12 bit resolution, this modest system will require 0.24 Mbits/s transfer rate. Hence, in one minute 14.4 Mbits are stored.

For a decent manufacturing process most of the times the strip will be defect free and, hence, the system output is not "interesting." Only when defects start occurring, the system output becomes interesting and it may contain information regarding the defects patterns that can be used to provide a feedback to the material grower for correction. This simple example shows that there is a need to compress the data at the hardware level to eliminate un-interesting stuff and to only look at the interesting portion of the data and the system output.

2. OPERATION PRINCIPLES

EMP is based on a resonator geometry shown in figure 1.a [1-3]. The reflection coefficient of this resonator is shown in figure 2. When an object is placed in the vicinity of the tip of the resonator (figure 1.b), both the resonance frequency (f_0) and the quality factor of the resonator (Q) are affected by the presence of the sample (figure 2). The amount of change in the resonance (Δf, and ΔQ) depends primarily on the microwave properties of the sample as well as on the distance between the resonator's tip and the sample (d), and the tip's effective area (A_{eff}). Keeping A_{eff} and "d" fixed, the tip can be scanned over the sample and variations in the sample's microwave properties can be mapped.

Figure 3 shows the electric field profiles and the magnitude of the current density distribution at 1 GHz determined using the full-wave analysis (using SONNET) of an evanescent microwave probe (EMP) (we use EMP and EMM interchangeably).

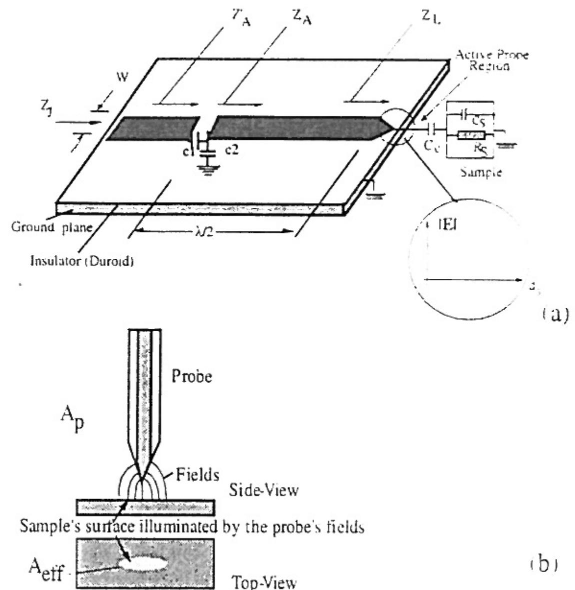

Figure 1 a) Microstripline resonator and probe assembly. Evanescent waves extend out of the tapered tip of the resonator. b) Schematic of probe field patterns and probe interaction with a sample.

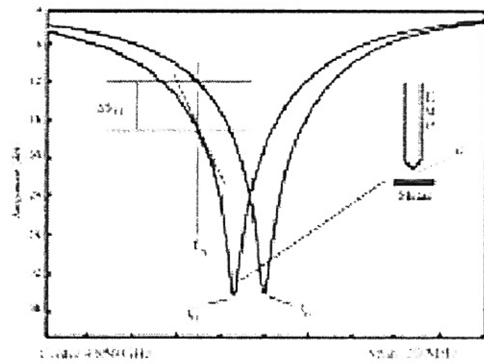

Figure 2 The resonance curve and its modification due to the presence of a metallic sample near the probe tip.

These figures show the confinement and the anisotropy of the fields near the probe tips. In the resistive sample, large magnitude of current densities are concentrated at the region closest to the probe tip as expected. Regions in the sample with considerable magnitude of current densities dominate the probe-sample interaction. From these figures it is clear that the interactions are localized at the vicinities of the probe tip regions indicating the origin of the high spatial resolution of EMP. In addition to tapering, and using a fine wire, attached to the tapered end of the

probe, an aperture can also be used to confine the fields at the probe tip.

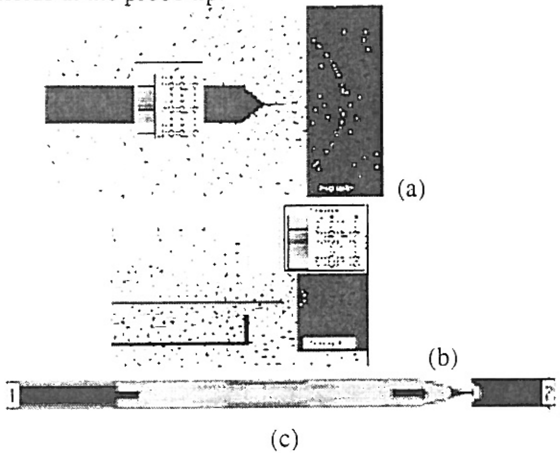

Figure 3 (a) Electric field intensity pattern showing the top view of the tapered probe. (b) Probe side view showing the anisotropic fields. (c) Current density obtained using SONNET in a resistive (16.77 Ω/square) sample.

We have used a variety of substrate materials including Duroid, SiO_2, Si_3N_4, and high-resistivity Si. Duroid substrates offer a wide range of relative permittivities and thickness. Higher permittivity substrates resulted in smaller line widths of the microstripline for 50 Ω characteristic impedance and have higher spatial resolutions.

3. EXPERIMENTAL PROCEDURE

The experimental set-up used in the present work is shown in figure 4, and it is similar to the set-up previously reported except for the addition of a rotational stage used for polar measurements [1-3]. The setup consists of a microwave resonator coupled to a feed-line (figure 1.a), which is connected to a circulator. The detector output is a DC voltage proportional to the magnitude of the reflected wave. This is fed to an amplifier and then to a lock-in amplifier. The probe is mounted vertically over a x-y stage (figure 4.b). The x-y stage and the frequency generator are controlled by a personal computer that also acquires data from the lock-in amplifier. Figure 4.b shows a photograph of the probe station.

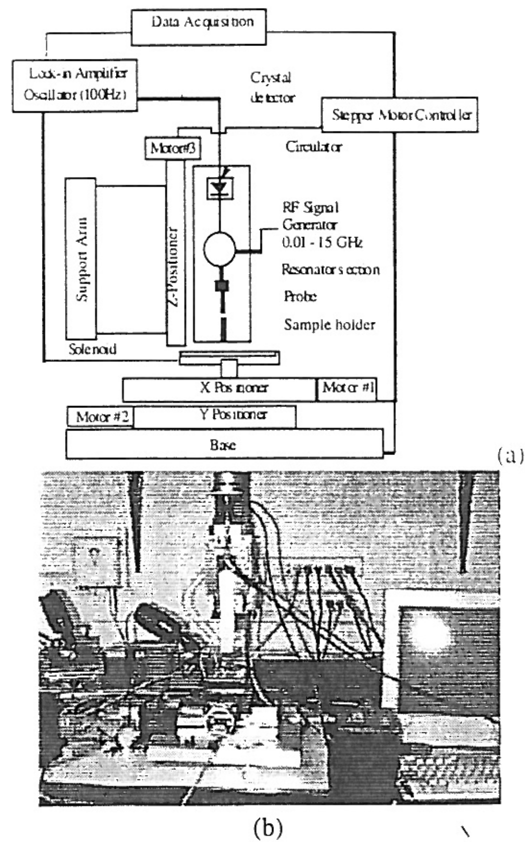

Figure 4 a) Schematic of the experimental set-up. b) Picture of the probe housing and the x-y-z polar scanner arrangement.

EMP Characteristics. The change in the EMP's output as a function of the tip-to-sample is nearly exponential with a decay length ((ξ^{-1}) of around 20 μm. The decay length (ξ^{-1}) and the lateral resolution of the EMP are related. ξ^{-1} depends on the tapering angle of the resonator (see figure 1.a), the length and diameter of the wire tip attached to the resonator, the resonator's substrate dielectric constant and thickness, the operation frequency, and the coupling strength between the resonator and the feed-line section.

Atomic Resolution. Figures 5.a and 5.b show100Å x 100Å 2-dimensional scans of a gold sample that were simultaneously obtained using the STM and the EMP. We used a STM probe (coupled with an evanescent microwave probe) to scan the gold sample. The two pictures are very similar indicating the atomic resolution of the EMP.

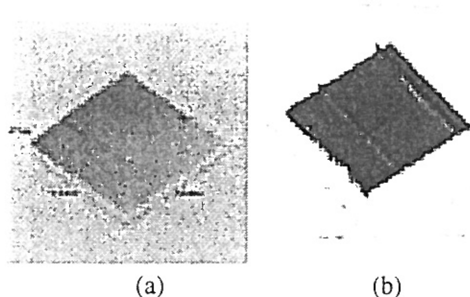

(a) (b)

Figure 5 100Å x 100Å simultaneous 2-D scan of a gold sample by (a) STM and (b) EMP showing the atomic resolution capability of the EMP. The line-width in these scan was 2.5 Å.

Calibration of EMP. To perform quantitative mapping of the conductivity, we calibrated the probe over a wide range of sheet resistance, from 0.24 Ω/Square to 65 kΩ/Square (figure 6). In our experiment, we used a Signatone 4-point probe, together with a Keithley 182 Sensitive Digital Multimeter and a 202 Programmable Current Source, to measure the sheet resistance of different samples. With this highly sensitive setup, a change of 10^{-4} in sheet resistance could be detected, and the deviation was below 2%.

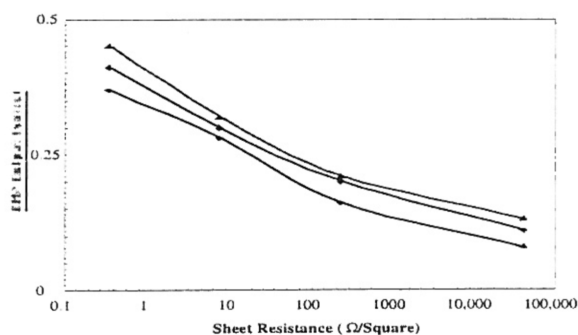

Figure 6 EMP calibration curves.

Polarization Data. Figure 7 shows polar scans of a thin-film YBCO sample, a polycrystalline PZT sample and a 12.5 μm wire. Wire being the most anisotropic sample has the largest EMP versus angle variations. The PZT sample having very small grain size (<1 μm) has some anisotropy. The thin-film YBCO sample had around 20 μm grain size and it was grown in the c-axis direction. The polar EMP shows the a-b axis anisotropy of the YBCO's conductivity at room temperature.

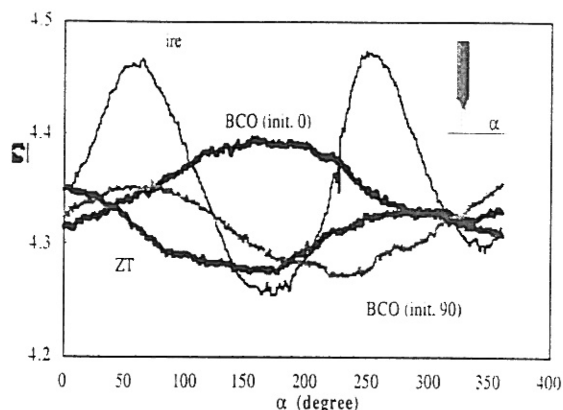

Figure 7 Polar EMP scans of different sample.

Microwave Images of Materials

Dielectrics. Figures 8.a and 8.b respectively show a photograph and the EMP image of an "x"' keypad of a calculator. Since the "x"' character was at the same level as the top surface of the pad, this figure clearly shows the ability of the EMP in detecting different dielectric regions. The "white" region in this pad had higher permittivity (by approximately factor of 2) than the "dark" region. Using the ability of the EMP to differentiate between different dielectric regions we have studied delamination in composites and defects in BN slabs in the past [1].

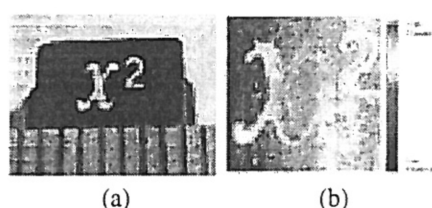

(a) (b)

Figure 8 Photograph (a) and EMP image (b) of an "x^2" key pad of a calculator.

Semiconductors. Figure 9 shows a 2-dimensional pseudo-colored scan of a 3" dia. Metal-organic 3C-SiC on Si wafer. The light spots are regions of lower resistivity (by as much as 10 times lower) caused by uneven gas flow patterns during the film growth. Since the microwave probe response is quite fast (<0.1 μs), the response of the semiconductor to an external stimulus, such as an optical pulse or a depleting high-power electromagnetic pulse, can be monitored. We have measured carrier recombination

lifetime in Si, GaAs, and InP using the EMP in the past.

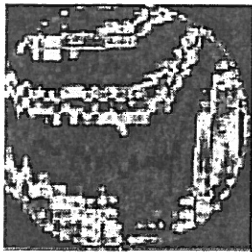

Figure 9 The EMP image of a 3" metal-organic SiC on Si clearly showing the doping nonuniformities due to uneven gas flow pattern during growth.

Metals. In figures 10.a and 10.b we have a photograph and the EMP image of a metallic pattern on a PC board, respectively. The EMP can image possible discontinuities in PC metallic lines and it can delineate spots of stressed regions. In figure 10.c a photograph and the EMP image of a CWRU medal is shown. The metallic letters had nominally 25 μm linewidths (as measured using an optical microscope) and could be easily detected using the microwave probe.

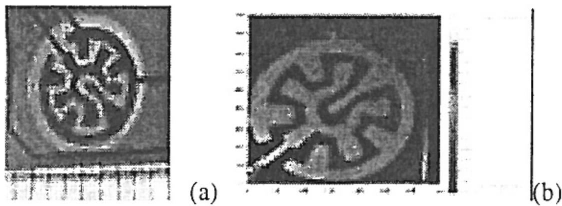

(c)

Figure 10 The photo (a) and EMP image (b) of the metallic pattern on a PC board (scale underneath the photo is in mm). (c) Optical image and EMP scan of a CWRU medal.

4. Parallel MEMS Probes and Data Management

The operation frequency of the EMP is very high (1-10 GHz has been demonstrated by our group). Thus, EMP's can have very fast scanning speeds. The imaging speed of the EMP can be further increased by using parallel probes to reduce the scanning time needed in covering large areas. Figure 11.a shows a possible application of parallel EMPs in an electronic thin-film manufacturing environment where the material is inspected immediately after deposition to detect any "fatal" flaws. The microwave imaging system is much more desirable than other indirect imaging techniques such as in-situ x-ray or high-resolution optical imaging because these other techniques do not image the "electrical" characteristics of the material directly.

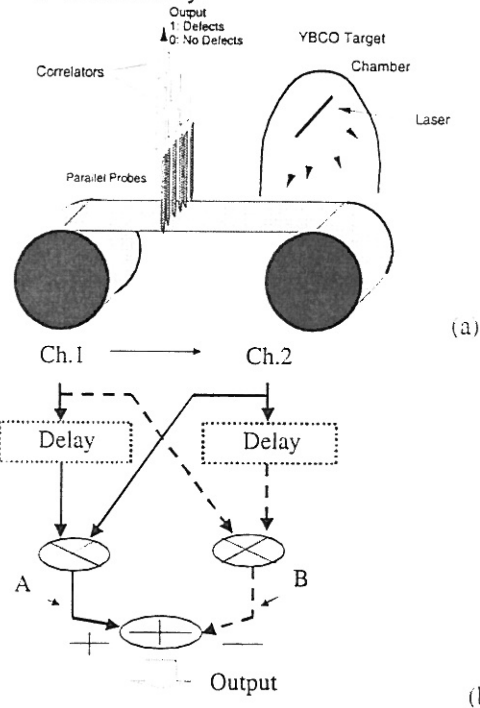

Figure 11 a) Schematic of the pulsed laser deposition chamber, the material tape and the EMP array to provide a feedback on the deposition quality. b) A correlator cell that is used to compare the probes output and to decide if the material is acceptable.

Neuromorphic Electronics. A defect detection imaging station is more desirable than a general purpose imaging system in the above situations. There are ample examples of such systems in the nature. For example, the human eye is an excellent example of "edge" detection system and it performs the edge detection locally without the help of the visual cortex. In insects, the complex eye is an excellent example of direction and speed detection system. Neuromorphic electronics reduces the computation overhead by locally processing the data and when used with "low

power" electronics it results in a considerable reduction in processing time and power consumption.

Figure 11.b shows an example of a neuromorphic "correlator" that is used to model the direction and pattern detection in certain insects. It can be adopted for our application in the following manner. We note that when defects start occurring they occur with some similarities. Thus, the correlator shown in figure 11.b can be used to combine the output of many sensors to detect these occurrences. The speed of the material tape is constant and defects may occur at different intervals. However, when fatal defects occur, they cover the width of the tape with some density larger than a threshold density. Thus, the delay in the correlator should be adjusted to detect the threshold density and to comply with the statistics of the defect occurrence that results in "unacceptable" material coverage.

Parallel Probes and Their Fabrications

Figure 12.a shows parallel probes with integrated tips. The top view of a single probe with microwave microstripline and the tip region is shown in figure 12.b. These probes are fabricated using low pressure chemical vapor deposited (LPCVD) polysilicon and deep reactive ion etching (DRIE). The details of fabrication will be discussed in a future publication. Both the integrated tip and the microstripline are functional. The Q of the probe resonators was around 10 and should be improved to improve the probe sensitivity.

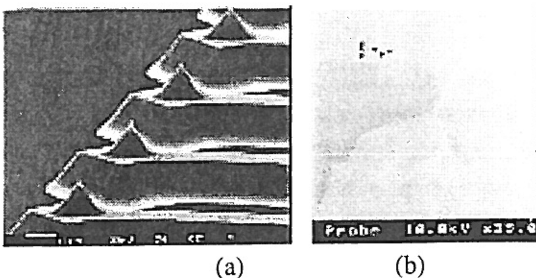

(a) (b)

Figure 12 Scanning electron microscope images of the parallel EMPs (a) and a single EMP with integrated microstripline and tip fabricated using polysilicon and deep reactive ion etching. The microstripline is formed by thin-film aluminum.

5. CONCLUSION

The main characteristics of a novel local probe that uses decaying, or evanescent, microwave fields to study materials is discussed. The main feature of these probes were their potentially high scanning speed, their hyperspectral imaging capabilities, and their atomic spatial resolution. It was also showed that a data compression method using neuromorphic electronics can be used to reduce the data bandwidth of parallel evanescent microwave probes and to increase its imaging and "flaw" detection speeds considerably.

Acknowledgment: The work reported here was partially supported by the Wright Patterson Air Force Base and Manufacturing Instrumentation Consultant Company (MICC). Mr. C. L. Shih of MICC fabricated probes shown in figure 12. Mr. R. Ciocan obtained figure 7. Mr. R. Muller and D. Su obtained figures 8 and 10.

6. REFERENCES

1. M. Tabib-Azar, **Evanescent Microwave Microscopy for High-Speed and High-Resolution Material Characterizations,** Kluwer Academic Pub., Boston (2000).
2. M. Tabib-Azar, N. Shoemaker and S. Harris, "Superresolution Characterization of Microwave Conductivity of Semiconductors." IOP Meas. Science Technology, Vol. 3, pp. 583-590 (1993).
3. M. Tabib-Azar, J. L. Katz, S. LeClair, "Evanescent Microwaves: A Novel, Super-resolution, Noncontact and Nondestructive Imaging Technique for Biological Applications." IEEE Trans. on Instrumentation and Measurement, p. 1111-1118 (1999).